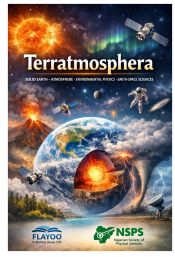
Produced and hosted by FLAYOO Publishing House LTD on behalf of the Nigerian Society of Physical Sciences (NSPS)

Terratmosphera

Solid Earth • Atmosphere • Environment • Space Sciences

https://flayoophl.com/journals/index.php/terratmosphera



Integrated geoelectrical and geotechnical characterization of subsurface conditions responsible for foundation failures at the former Shagari housing estate, Numan, Adamawa State, Nigeria

Beatrice Bomki Humphrey, Jamu Benson Yerima, Emmanuel Ike*, Adetola Sunday Oniku

Department of Physics, Faculty of Physical Sciences, Modibbo Adama University, Yola, Nigeria

ARTICLE INFO

Article history:
Received: 01 April 2026
Received in revised form: 16 April 2026
Accepted: 17 April 2026
Available online: 23 June 2026

Keywords: Foundation failure, Electrical resistivity tomography, Geotechnical characterization, Differential settlement

DOI:10.61298/terratmosphera.2026.1.1.346

ABSTRACT

Foundation failures remain a persistent challenge within heterogeneous basement-complex terrains of northeastern Nigeria. This study presents an integrated geoelectrical–geotechnical investigation of foundation failures at the former Shagari Housing Estate, Numan, Adamawa State, Nigeria, aimed at delineating subsurface conditions responsible for structural distress and differential settlement. Two-dimensional electrical resistivity tomography (ERT), acquired with the Wenner configuration and interpreted using RES2DINV inversion software, was combined with laboratory geotechnical analyses to develop a robust subsurface failure model. Geoelectrical results reveal very low resistivity values (2.67–24.7 Ω m), indicating water-saturated, weak clayey subsoils, with corrosivity conditions ranging from very strongly to moderately corrosive. Particle-size distribution shows high fines content (79.48%), exceeding the recommended 35% threshold. Atterberg limits confirm expansive behavior, with liquid limits of 49.00–56.80% and plasticity indices of 31.07–41.15%, while natural moisture contents (18.99–23.08%) exceed acceptable ranges. Undrained triaxial tests show low shear strength (cohesion: 7–22 kN/m^2; friction angle: 1.5°–5°) and low bearing capacity (maximum 55.16 kN/m^2). Consolidation results indicate medium to high compressibility and low permeability. The strong spatial correlation between low-resistivity zones and poor geotechnical properties confirms that the observed failures are associated with highly plastic, compressible, and moisture-sensitive soil layers. The findings demonstrate that integrating ERT with laboratory analyses provides a reliable predictive framework for identifying geotechnically vulnerable zones before construction.

© 2026 The Author(s). Produced and hosted by FLAYOO Publishing House LTD on behalf of the Nigerian Society of Physical Sciences (NSPS). Peer review under the responsibility of NSPS. This is an open access article distributed under the terms of the Creative Commons Attribution 4.0 International License, which permits unrestricted use, distribution, and reproduction in any medium, provided the original work is properly cited. Any further distribution must preserve attribution to the author(s), the article title, the journal citation, and the DOI.

1. INTRODUCTION

The persistent occurrence of structural failures in Nigeria particularly in regions with complex geological and geotechnical conditions, such as Numan in northeastern Nigeria has resulted in

*Corresponding author. Tel. No.: +234-806-2356-335.
e-mail: emmanuelike@mau.edu.ng (Emmanuel Ike)

significant economic losses and poses serious threats to human safety. A key factor influencing the stability and durability of buildings is the quality of the foundation. Foundation failure can have severe implications for both structural integrity and occupant safety, thereby affecting economic sustainability. Consequently, geophysical and geotechnical investigations are crucial for identifying the root causes of foundation failures and developing effective mitigation strategies. Foundations serve as the critical interface between civil engineering structures and the underlying soil, playing a fundamental role in transmitting structural loads to the ground and ensuring overall stability and support [1].

Foundation failure refers to the structural deterioration or collapse of a building's foundation, resulting in compromised stability and potential structural damage. It occurs when the foundation is unable to adequately support the imposed loads and stresses, leading to issues such as settlement, sinking, cracking, or displacement of the superstructure. This phenomenon can arise from a variety of factors, such as soil instability, poor construction practices, inadequate design, moisture-related problems, or a combination of these factors [2–4]. While improper design is a significant contributor, other deficiencies like situating a structure on unsuitable or weak soil layers also play a critical role in compromising the integrity of a building [4–7]. These unstable subsurface conditions can lead to differential settlement or even total structural failure. To prevent such outcomes, it is essential to assess the foundation's integrity and bearing capacity by thoroughly evaluating the subsurface soil characteristics and stratigraphy [2, 8, 9]. In this context, researchers often employ both geophysical and geotechnical investigation techniques to gather crucial information about the subsurface.

Geophysical methods like the electrical resistivity tomography (ERT) offers continuous, non-invasive subsurface imaging and delineation of subsurface conditions without compromising quality [4, 6, 10, 11]. By measuring variations in electrical resistivity across different soil layers, researchers can infer changes in soil composition, moisture content, detect potential subsurface geological features or anomalies such as voids or fractures and water saturation zones that might otherwise go undetected in point-specific geotechnical sampling [10–12]. This synergy enhances the accuracy and reliability of foundation assessments, reduces uncertainty, and leads to more efficient and cost-effective construction outcomes [2, 3, 5, 6, 8, 9] .

Several studies have demonstrated the effectiveness of integrating geophysical and geotechnical methods in diagnosing foundation-related problems. In a seminal review, Samouëlian *et al.* [13] synthesized the fundamental controls on soil resistivity, showing that parameters such as moisture content, clay fraction, porosity, and soil structure strongly influence electrical responses. They established that electrical resistivity methods, including 1D sounding and 2D/3D electrical resistivity tomography (ERT), as reliable, non-invasive tools for mapping subsurface heterogeneity, while emphasizing the need for calibration with direct measurements thereby laying the foundation for integrated geophysical–geotechnical applications.

Subsequent studies extended these principles to engineering and foundation investigations. Sudha *et al.* [2] demonstrated that resistivity methods effectively delineate lithological variations and identify weak, water-saturated zones that may compromise foundation stability. Similarly, Obasi *et al.* [14] showed that Vertical Electrical Sounding (VES) can distinguish competent lateritic and sandstone units from weak clay/shale sequences, providing a cost-effective basis for site characterization in tropical sedimentary environments. Devi *et al.* [3] further confirmed that low resistivity values are associated with weak, fine-grained, moisture-rich soils with low shear strength, and highlighted that integrating resistivity imaging with geotechnical data significantly improves the delineation of weak zones both laterally and vertically. Odundun *et al.* [15] documented widespread foundation problems linked to clay-rich soils and shallow groundwater conditions, reinforcing the importance of combined geoelectrical and geotechnical investigations for appropriate foundation design. Likewise, Atilade *et al.* [5] attributed frequent building collapse in Lagos Nigeria to low-resistivity, clayey subsurface materials, underscoring the engineering implications of such weak zones. Beyond terrestrial settings, Bellmunt *et al.* [16] demonstrated the applicability of electrical resistivity tomography (ERT) in complex saline deltaic environments, emphasizing the need to integrate geophysical data with geological information where resistivity contrasts are subdued by pore-water salinity.

More studies have focused on strengthening the quantitative integration of geoelectrical and geotechnical data. Sharma *et al.* [9] established that higher resistivity values generally correspond to denser and more competent soils, while stressing that reliable interpretation requires site-specific calibration due to geological variability. Adewoyin *et al.* [17] further demonstrated that geophysical data can be used to estimate key geotechnical parameters, providing a cost-effective alternative for preliminary site assessment. Additional studies reinforce the growing importance of integrated approaches. Aguirre-Macías *et al.* [6] showed that standardized resistivity–geotechnical relationships enhance the reproducibility of ERT-based site characterization, particularly in data-sparse urban environments. Erick *et al.* [10] emphasized that geophysical methods, especially ERT, provide spatially continuous data that complement point-based geotechnical tests, enabling better characterization of subsurface heterogeneity, which is an essential factor controlling foundation performance.

Collectively, the reviewed studies demonstrate that weak, clay-rich, saturated, and moisture-sensitive subsurface conditions constitute major predisposing factors to foundation failure. The evidence further underscores that the integration of geophysical and geotechnical techniques offers a robust and reliable scheme for detailed subsurface characterization and informed, sustainable foundation design.

Most structures in Numan, particularly within the Former Shagari Housing Estate, exhibit clear signs of foundation failure, including extensive cracking, tilting, and, in some cases, complete collapse (Figure 1). Despite the prevalence of these structural deficiencies, no comprehensive study has systematically investigated their underlying causes. This study therefore seeks to address this gap by integrating geoelectrical and geotechnical approaches to provide a robust evaluation of subsurface conditions, recognizing that reliance on a single method may yield incomplete or potentially misleading interpretations.

The electrical resistivity method, specifically the Wenner configuration, was adopted due to its ability to capture both verti-

cal and lateral variations in resistivity [3, 4, 18, 19], in addition to its high signal-to-noise ratio and effectiveness in resolving near-surface anomalies [4]. Complementarily, geotechnical samples were collected at a depth of 2 m across selected locations, guided by resistivity results to ensure representative coverage of soil strata susceptible to shear and consolidation under structural loads, thereby improving settlement prediction [16].

Ultimately, the findings of this study will support the rehabilitation of existing structures and inform the design and planning of future infrastructural developments, thereby improving structural durability and sustainability. More broadly, the results contribute to safer engineering practices, reduced economic losses, advancement of geotechnical knowledge, and sustainable urban development, while serving as a valuable reference for similar environments.

2. LOCATION AND GEOLOGY OF THE STUDY AREA

The study area is located at the Former Shagari Housing Estate in Numan, Adamawa State, northeastern Nigeria (Figure 2). The area is situated within the Benue River valley, a major physiographic feature in northeastern Nigeria, which significantly influences the geomorphology and sedimentation patterns of the region [20–22].

Geologically, the study area falls within the Upper Benue Trough, a major intracratonic rift basin that extends across northeastern Nigeria and forms part of the West and Central African Rift System [21, 22]. The Benue Trough is characterized by thick sequences (up to about 6000 m) of Cretaceous sediments (Figure 3), including continental, transitional, and marine deposits that have undergone deformation and tectonic modification [20, 21].

The dominant lithostratigraphic unit in the area is the Bima Formation, which represents the oldest sedimentary sequence within the Upper Benue Trough. The Bima Formation consists predominantly of sandstones, siltstones, and intercalated clay layers deposited in continental environments during the Early Cretaceous [21]. Sedimentological studies indicate that these deposits were formed in fluvial to alluvial systems, with facies associations ranging from braided-channel sand bodies to floodplain deposits [20–22]. The sediments are generally poorly sorted and texturally immature, reflecting deposition close to their source terrains [21]. The development of the Bima Formation and associated sedimentary sequences was controlled by Early Cretaceous rifting, which produced a system of horsts and grabens that influenced sedimentation and basin architecture [24] . The sediments were largely derived from adjacent Precambrian Basement Complex rocks, including the Adamawa Massif and surrounding highlands [20, 21]. Generally, the geological setting of the study area reflects a complex interaction of fluvial-alluvial deposits, Cretaceous sedimentary formations, and weathered basement materials.

3. MATERIALS AND METHODS

3.1. GEOELECTRICAL DATA ACQUISITION AND PROCESSING

3.1.1. Materials for the geoelectrical investigation

The materials used for electrical resistivity data acquisition and positioning were as follows.

Earth Resistivity Meter (Terrameter).

The terrameter was the core instrument used to measure subsurface resistivity. It injects electrical current into the ground through current electrodes and records the resulting potential difference across potential electrodes . These measurements are used to compute apparent resistivity , which forms the basis for the subsurface imaging.

Electrodes.

Metal electrodes were inserted into the ground to establish electrical contact. Two electrodes serve as current injectors , while the other two measure potential differences . Proper grounding ensures accurate and stable data acquisition.

Cable Reels and Connecting Wires.

Multi-core cables and reels were used to connect the electrodes to the terrameter. They enable systematic electrode arrangement along the traverse line and ensure efficient transmission of electrical signals during the survey.

Measuring Tape.

A measuring tape was used to accurately space the electrodes (2 m interval in this study) along each traverse line. Precise spacing is essential for maintaining the integrity of the Wenner configuration and ensuring reliable data.

Hammer (or Mallet).

A hammer was used to drive the electrodes into the ground to achieve firm contact, particularly in compact or dry soils where penetration may be difficult.

Global Positioning System (GPS) Device.

A Global Positioning System device was used to record the geographic coordinates and elevation of each survey location. This ensures proper spatial referencing of the data for interpretation and mapping.

Field Recording Materials.

Field notebooks, data sheets, or digital logging systems were used to document measurements, electrode positions, site conditions, and other relevant observations during the survey.

Together, these materials enable accurate acquisition, positioning, and documentation of resistivity data, which is essential for generating reliable subsurface models and interpreting geological conditions relevant to foundation stability.

3.1.2. Method for the geoelectrical survey

The study employed two-dimensional (2D) electrical resistivity imaging using the Wenner configuration to characterize subsurface conditions. This configuration comprises four (4) collinearly arranged electrodes with equal spacing, in which the outer pair functions as current electrodes (C_1 and C_2) and the inner pair as potential electrodes (P_1 and P_2). Data acquisition was conducted along four (4) traverses using a constant electrode spacing of 2 m, providing a high signal-to-noise ratio and strong sensitivity to vertical resistivity variations. These characteristics make the Wenner array particularly effective for resolving near-surface stratification and identifying geoelectrical contrasts or



(a) (b)

Figure 1. Common structural distress observed in buildings within the study area: (a) cracks on building walls, indicating differential settlement and foundation instability, and (b) dilapidated structures resulting from prolonged structural weakening and inadequate ground support.

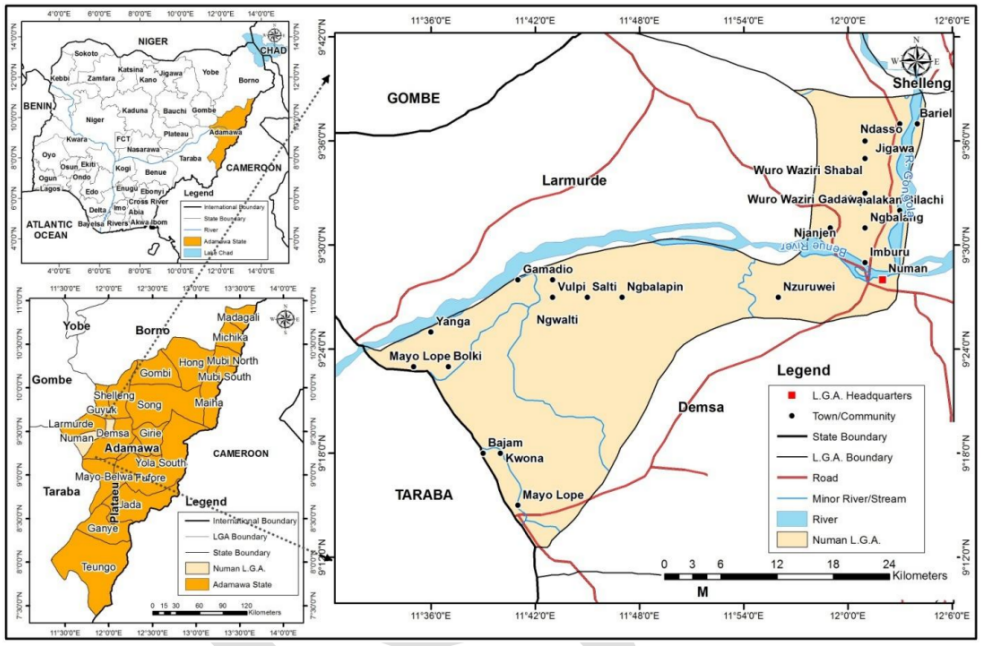


Figure 2. Location map of Numan, Adamawa State, Nigeria [23].

anomaly associated with variations in soil composition, moisture content, and structural integrity [11–13, 25].

The Wenner configuration was selected for its balanced sensitivity to both vertical and lateral resistivity variations, its high data quality, and its effectiveness in resolving shallow subsurface anomalies relevant to foundation studies [4, 11, 19]. These attributes make it well suited for assessing subsurface conditions that influence building foundation integrity. The electrical resistivity data were processed using RES2DINV software, a specialized inversion tool that applies forward modelling to simulate subsurface current flow based on an initial resistivity model, followed by iterative refinement to minimize the misfit between measured and calculated data. The final output is a two-dimensional resistivity model presented as colour-coded pseudo-sections, illustrating subsurface variations to a depth of approximately 10 m. Interpretation was further supported by correlating the results with established resistivity signatures of local soils and geological formations in the study area.

3.2. GEOTECHNICAL DATA ACQUISITION AND PROCESSING

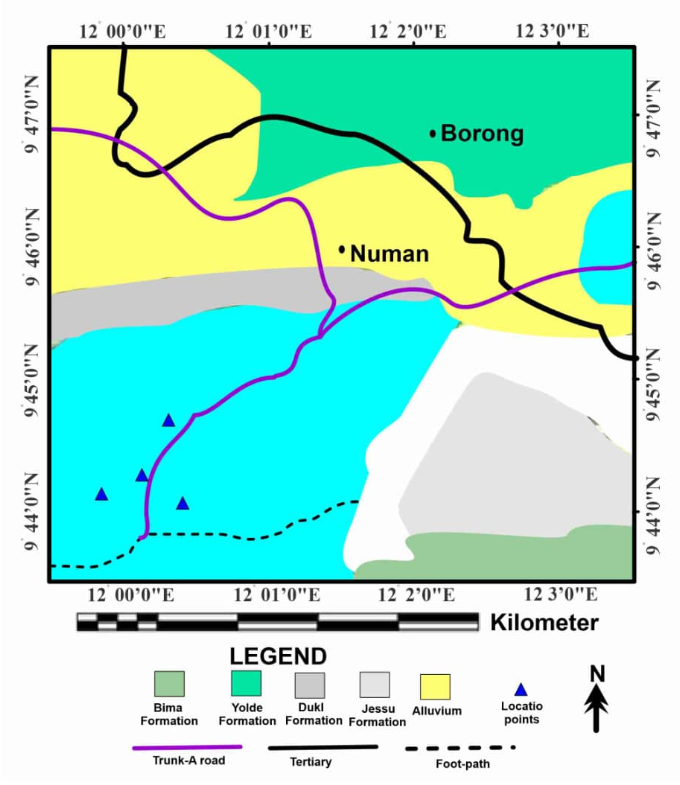


Figure 3. Geological map of Numan showing the spatial distribution of major lithological units, including alluvial deposits, Bima Formation sandstones, and underlying basement complex rocks.

3.2.1. Materials for the geotechnical survey

The materials used for geotechnical data acquisition and positioning were as follows.

Sampling Tools (Auger/Hand Tools).

Soil samples were collected using hand tools and augers to a depth of 2 m. These methods facilitate the recovery of both disturbed and undisturbed, representative samples from subsurface layers relevant to foundation conditions.

Polyethylene sample bags.

Airtight polyethylene bags were used to store the collected samples. These prevented moisture loss and contamination, thereby preserving the natural condition of the soil prior to laboratory testing.

Global positioning system (gps) device.

A Global Positioning System device was used to record the coordinates of each sampling location. This ensures proper spatial referencing and correlation with geophysical data.

Field recording materials.

Field notebooks, labels, and markers were used to document sample locations, depths, and site observations. Proper documentation is essential for traceability and data integrity.

Table 1. Coordinates of the sample points in this study.

Sample point	Latitude (N)	Longitude (E)
A	9.442117°	12.006705°
B	9.443222°	12.008414°
C	9.442458°	12.009174°
D	9.443218°	12.010248°

Sieve set (for particle size analysis).

A standard set of sieves was used to determine the grain size distribution of the soil. This helps classify the soil and assess its engineering behavior, such as permeability and compaction characteristics.

Moisture content apparatus.

Equipment such as moisture cans, weighing balance, and drying oven were used to determine the natural moisture content of the soil. This parameter is critical in evaluating soil consistency and strength.

Triaxial compression apparatus.

The triaxial testing machine is used to determine the shear strength parameters of the soil under controlled stress conditions. It provides insights into soil behavior under loading, which is essential for foundation design.

Consolidation (oedometer) apparatus.

This apparatus is used to perform one-dimensional consolidation tests, which evaluate the compressibility and settlement characteristics of the soil under applied loads.

Atterberg limits test.

Devices such as the liquid-limit apparatus and plastic-limit tools were used to determine the consistency limits of fine-grained soils. These limits are important for soil classification and predicting engineering performance.

Weighing balance.

A sensitive balance was used in multiple tests (moisture content, sieve analysis, Atterberg limits) to obtain accurate mass measurements required for calculations.

Drying oven.

A laboratory oven was used to dry soil samples at controlled temperatures, particularly for moisture content determination and sample preparation. These materials collectively enabled accurate sampling, preservation, and laboratory characterization of the soils. The resulting data are essential for evaluating soil strength, compressibility, and overall suitability for supporting engineering structures.

3.2.2. Method for the geotechnical survey

A total of four (4) disturbed and undisturbed soil samples were collected from a depth of 2 m at strategically selected locations within the study area (Table 1). This sampling depth exceeds the typical foundation embedment depth for low-rise structures (~ 1 – 1.5 m), thereby ensuring that the retrieved samples adequately

represent subsurface strata that are critical to foundation performance, including layers prone to shear failure and consolidation. To enhance spatial representativeness and reduce interpretational uncertainty, the selection of sampling points and depths was guided by prior geoelectrical resistivity results, enabling targeted investigation of zones exhibiting anomalous subsurface conditions, consistent with integrated geoelectrical–geotechnical approaches reported in recent studies [2, 3, 9]

The collected samples were immediately sealed in airtight polyethylene bags to preserve their in situ moisture conditions and subsequently transported to the Geotechnical Engineering Laboratory, Department of Civil Engineering, Modibbo Adama University, Yola, for detailed analysis. Laboratory testing was conducted in accordance with established international standards, including ASTM D2487-11 and relevant British Standard procedures, which are widely applied in geotechnical investigations and underpin reliable soil classification and engineering characterization [13, 27–29].

The suite of laboratory tests performed comprised particle size distribution (sieve analysis), natural moisture content determination, Atterberg limits, undrained triaxial compression testing, and one-dimensional consolidation tests. These tests provide a comprehensive evaluation of the soils' index properties, strength characteristics, and compressibility behavior, which is essential for assessing their suitability for foundation support and predicting settlement behavior. Similar testing frameworks have been widely adopted in recent high-impact studies integrating laboratory and field data for foundation assessment and subsurface characterization [17, 26, 27] .

A schematic diagram of the methods adopted in this study is as shown in Figure 4.

4. RESULTS AND DISCUSSION

4.1. ELECTRICAL RESISTIVITY SURVEY

The results of the two-dimensional (2D) electrical resistivity surveys conducted along the four (4) profiles are illustrated in Figures 5, 6, 7 and 8. The resistivity model for Profile 1 (Figure 5) reveals predominantly low resistivity zones (2.67–24.7 Ωm) within the near-surface layers, indicating weak, clay-rich, and possibly water-saturated materials. These zones are laterally continuous and extend to depths of approximately 10 m, suggesting poor competence and high susceptibility to settlement and foundation instability.

Similar to Profile 1, Profile 2 (Figure 6) is characterized by low resistivity values (2.91–17.1 Ωm), indicating the dominance of conductive materials such as clay and silty clay. The persistence of these low-resistivity zones suggests weak subsurface conditions that may adversely affect load-bearing capacity and structural stability.

The resistivity distribution for Profile 3 (Figure 7) further confirms the prevalence of conductive (2.91–17.3 Ωm), fine-grained materials. The close agreement between measured and calculated data indicates good inversion quality, while the resulting model highlights zones of potential weakness associated with saturated or clayey formations.

Profile 4 (Figure 8) also exhibits low resistivity values (3.39–17.4 Ωm), consistent with the other profiles. These results indicate laterally extensive weak zones and reinforce the interpretation of poor foundation conditions across the study area.

Across all profiles (Figures 5–8), resistivity values can be broadly classified into low (blue), medium (green–yellow), and high (red–purple) zones. Resistivity values below 30 Ωm are generally indicative of weak zones [4, 30], suggesting that the corresponding sections in Profiles 1–4 are geotechnically incompetent for construction and are likely contributors to the observed structural failures. As reported by Audu *et al.* [4] and Atilade *et al.* [5], low-resistivity anomalies are commonly associated with geological features such as faults, fractures, moist clay-rich zones, silty sand, sandy clay, and other unconsolidated subsurface materials, all of which adversely affect foundation stability.

Moreover, the presence of ions and electrolytes in pore water significantly reduces resistivity values [18], thereby enhancing soil instability and promoting erosion-prone conditions [13, 28]. This interpretation is consistent with the findings of Bisong *et al.* [30], who linked low resistivity anomalies to structurally weak zones. Consequently, soils exhibiting such characteristics are generally unsuitable for supporting foundations, as they are prone to differential settlement and structural damage, including wall cracking [31].

In particular, silty soil mixtures as observed are characterized by weak inter-particle bonding and loose structure, resulting in low shear strength and poor load-bearing capacity [28]. Although sandy soils exhibit high permeability, which enhances drainage and reduces waterlogging, their non-cohesive nature, makes them susceptible to displacement and erosion. The electrical resistivity of sand–silt mixtures is therefore highly variable, being controlled by factors such as moisture content, porosity, temperature, and dissolved salt concentration. In all, the observed resistivity patterns align with previous studies that associate low resistivity with clay-rich formations, fractures, and water-saturated zones, all of which contribute to reduced geotechnical competence [4, 5].

Furthermore, the subsurface soils within the study area were classified based on their corrosivity potential (Table 2) using the criteria of Akinlabi and Olaiya [32], and Amadi *et al.* [33]. Soil corrosivity describes the capacity of subsurface materials to promote electrochemical degradation of buried metallic components, particularly reinforcement steel, pipelines, and grounding systems. From a geotechnical–geophysical standpoint, low resistivity values are widely interpreted as indicators of aggressive soil environments, typically associated with elevated moisture content, high ionic concentration, reduced oxygen diffusion, and a dominance of clay-rich fine-grained materials. These conditions enhance electrical conductivity and accelerate electrochemical corrosion processes within the soil matrix [13] .

According to established geoelectrical classification schemes, soils with resistivity values below 10 Ωm are classified as very strongly corrosive, values between 10 and 60 Ωm indicate moderately corrosive conditions, values ranging from 60 to 180 Ωm suggest slight corrosivity, whereas values above 180 Ωm correspond to low- to non-corrosive environments [31–33]. The resistivity values obtained in this study (2.67–24.7 Ωm) therefore indicate that the subsurface conditions are predominantly moderate to very strongly corrosive. Consequently, the study area is largely characterized by moderate to high corrosion potential zones.

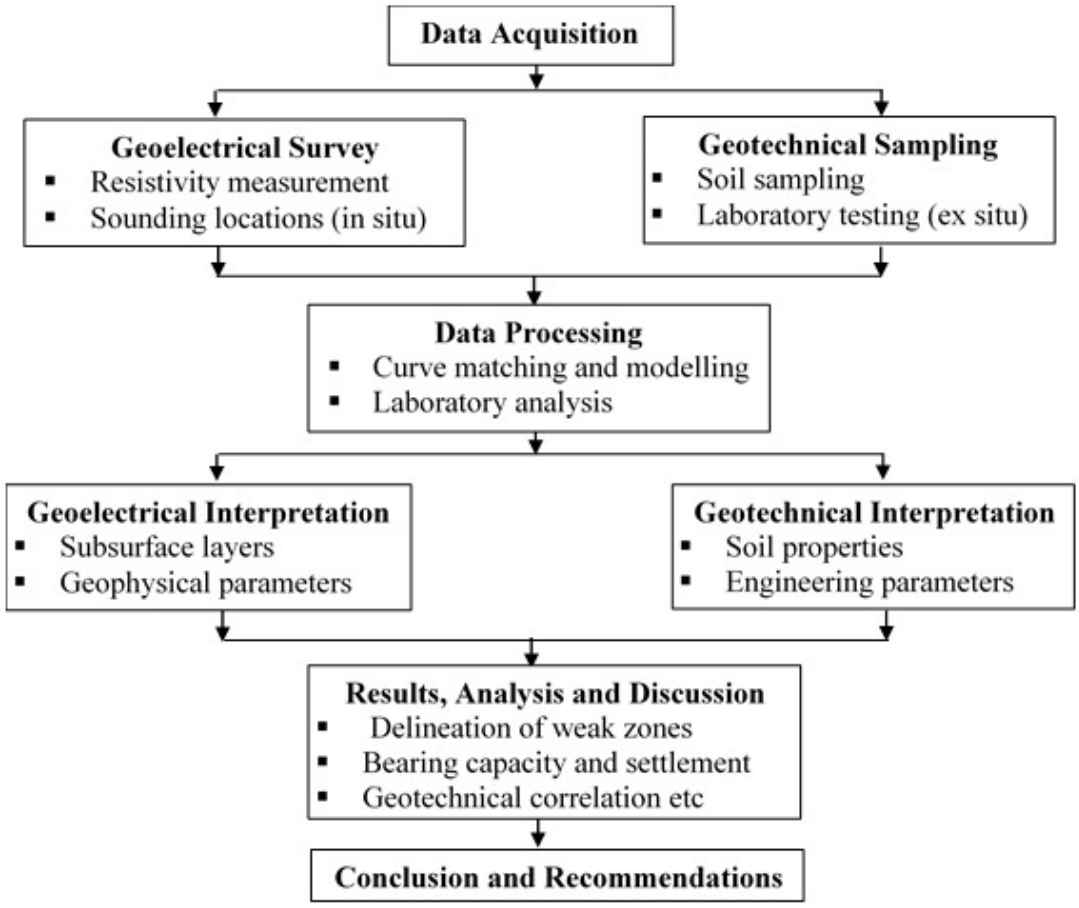


Figure 4. Schematic diagram of the methodology adopted in this study.

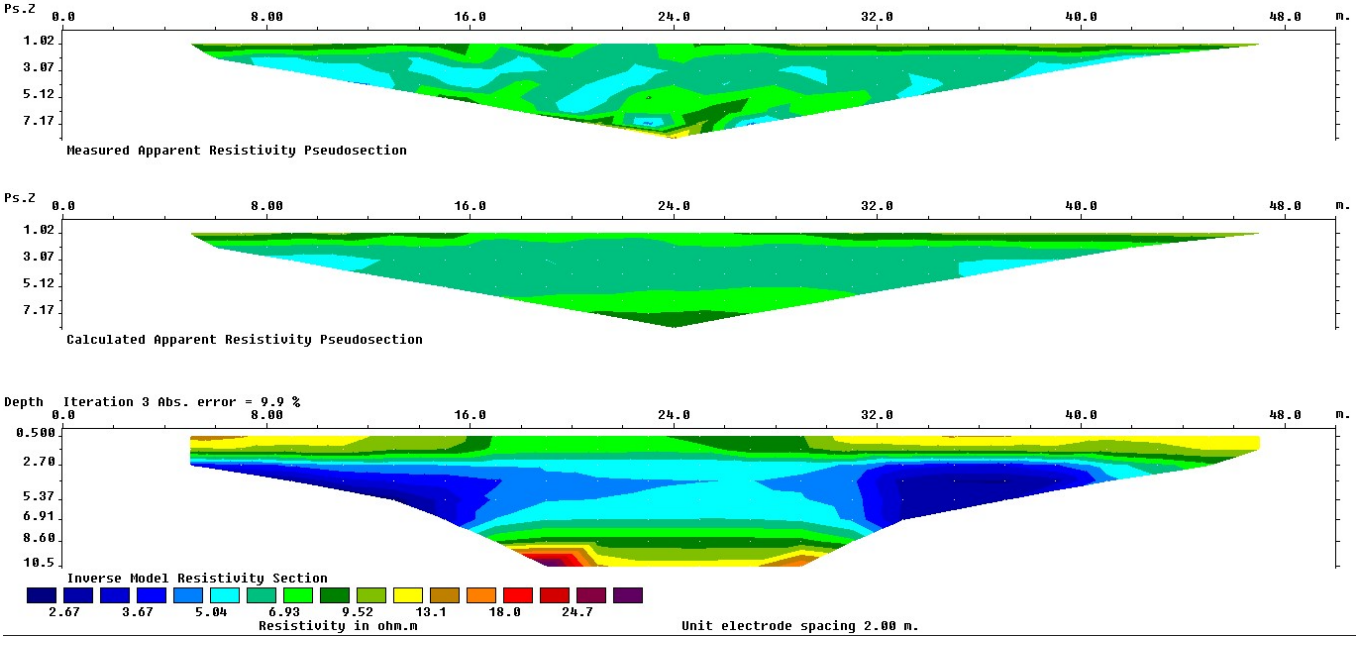


Figure 5. Pseudo-section plots for Profile 1 showing measured apparent resistivity, calculated apparent resistivity, and inverted model resistivity distribution.

Corrosion of reinforcement steel in such environments typically leads to a progressive reduction in the steel's cross-sectional area, cracking and spalling of the concrete cover due to the expansive nature of corrosion products, deterioration of the steel–

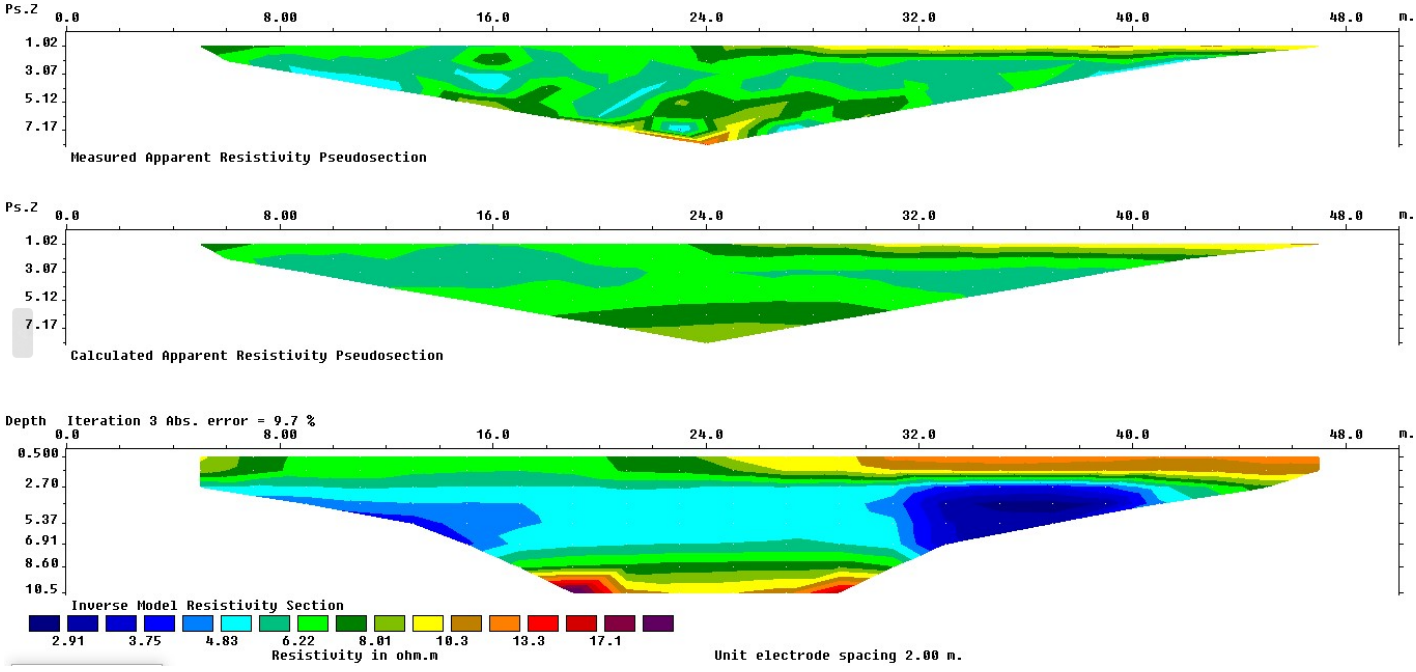


Figure 6. Pseudo-section plots for Profile 2 showing measured, calculated, and inverted resistivity distributions.

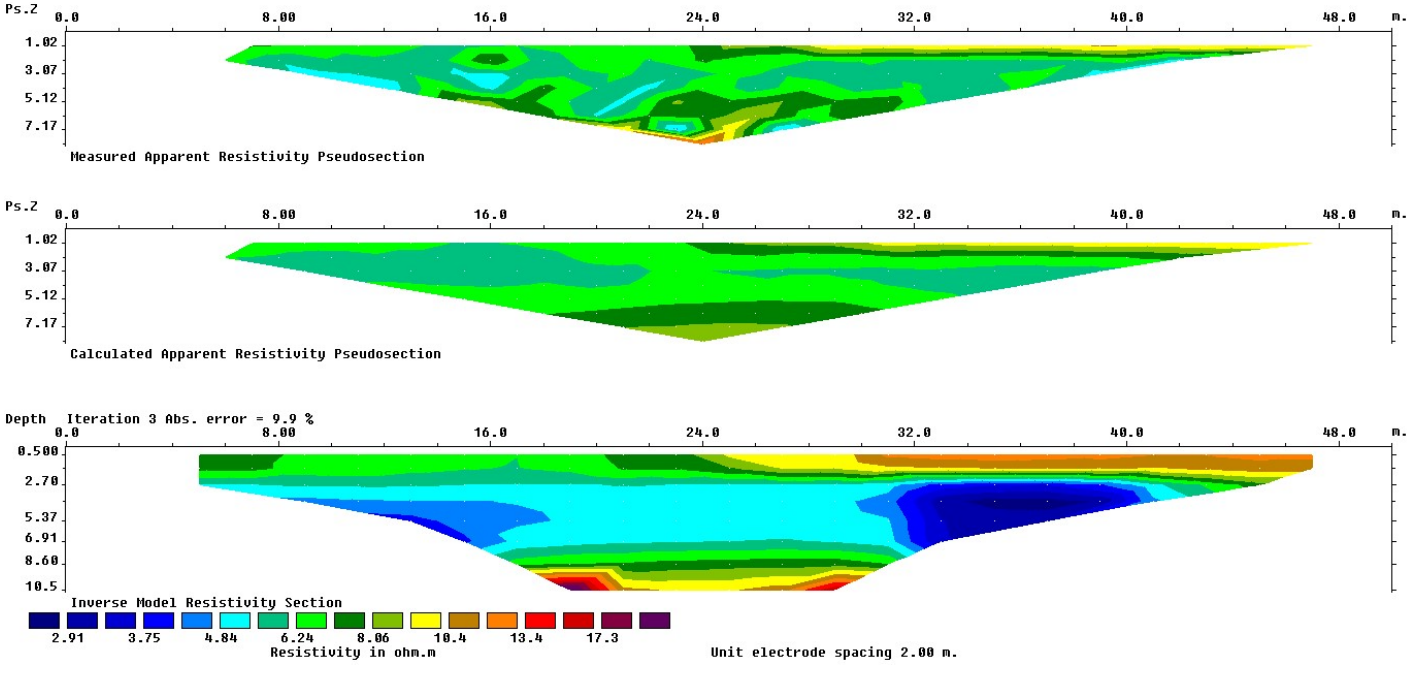


Figure 7. Pseudo-section plots for Profile 3 showing measured, calculated, and inverted resistivity distributions.

concrete bond, compromised structural integrity and long-term durability of reinforced concrete systems, ultimately and a resulting decline in the load-bearing capacity of the structure. Therefore, without appropriate mitigation measures such as soil stabilization, protective coatings, cathodic protection, and the adoption of properly designed deep or raft foundation systems, the study area may be highly susceptible to structural degradation and long-term infrastructure failure.

4.2. GEOTECHNICAL ANALYSIS

4.2.1. Natural moisture content (NMC)

The natural moisture content (NMC) of the soil samples, as presented in Table 3, ranges from 18.99% to 23.08%, indicating relatively high values. This range exceeds the recommended 5%–15% limit for soils in Nigeria as widely benchmarked against the Federal Ministry of Works and Housing standards [4, 26] and against general clay behavior, plasticity & engineering properties [8, 29], thereby classifying all the collected samples as unsuitable for direct use in construction. Soils with high moisture content, particularly those that are saturated or near-saturated, are more

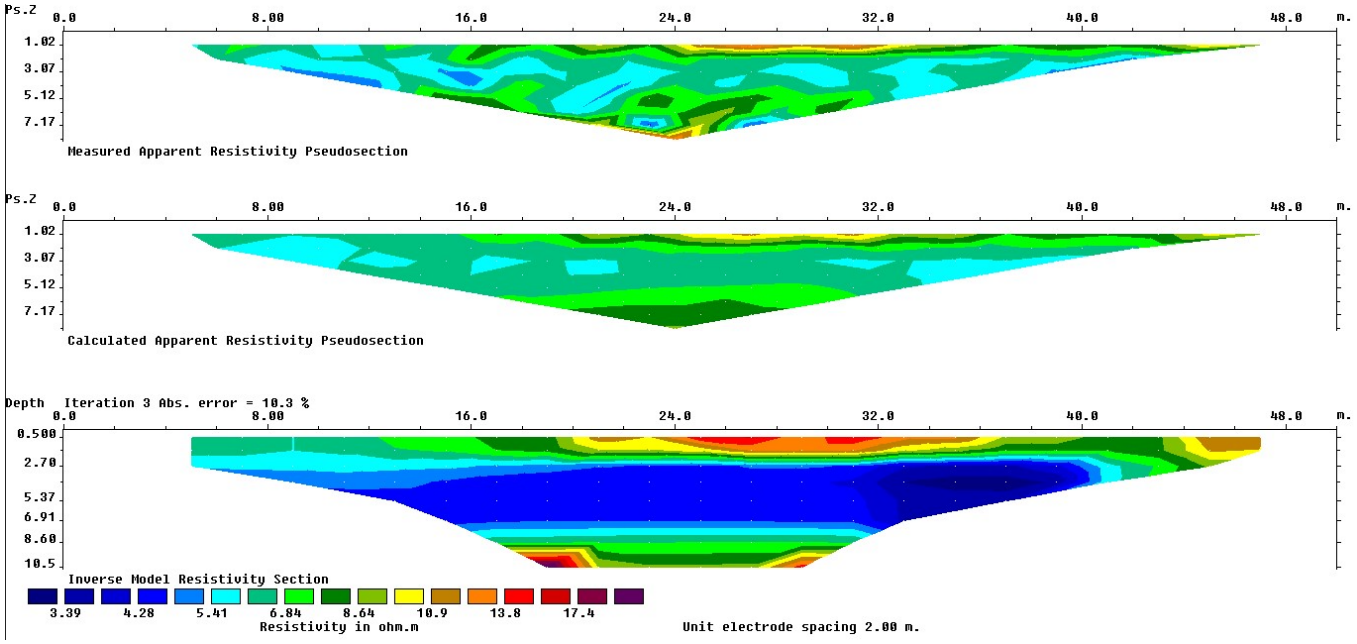


Figure 8. Pseudo-section plots for Profile 4 showing measured, calculated, and inverted resistivity distributions.

Table 2. Classification of soil resistivity in terms of corrosivity [31–33].

S/No.	Range of soil resistivity (Ω m)	Study area (Ω m)	Description
1	Less than 10	2.67–24.7	Very strongly corrosive
	10–60	2.67–24.7	Moderately corrosive
2	Less than 10	2.91–17.1	Very strongly corrosive
	10–60	2.91–17.1	Moderately corrosive
3	Less than 10	2.91–17.3	Very strongly corrosive
	10–60	2.91–17.3	Moderately corrosive
4	Less than 10	3.39–17.4	Very strongly corrosive
	10–60	3.39–17.4	Moderately corrosive

susceptible to compression under applied loads, which can lead to excessive settlement of foundations and structural instability [5].

The observed unsuitability of these soils highlights the need for appropriate ground improvement measures. Such measures may include soil replacement or stabilization using additives such as lime or cement, incorporation of geotextiles, provision of efficient drainage systems to minimize water retention, and strict compaction control during construction.

4.2.2. Consistency limits

The consistency limits of the soil samples, as presented in Table 4, indicate that the liquid limit (LL) ranges from 49.00% to 56.80%, the plastic limit (PL) from 14.10% to 20.87%, and the plasticity index (PI) from 31.07% to 41.15%. Soils with liquid-limit values less than 30% are generally classified as low plasticity, those between 30% and 50% as medium plasticity, while soils with liquid limits exceeding 50% are considered highly plastic or fat clays [28, 29]. Based on this classification, the soils in the study area predominantly fall within the medium to high plasticity range, with most samples (A, B, and C) exceeding the 50% threshold, indicating a dominance of high-plasticity clay [5, 7].

For satisfactory performance in construction applications, recommended limits typically include a liquid limit below 35% and a plasticity index below 12% [26, 34]. The values obtained in this study significantly exceed these thresholds, suggesting poor engineering properties such as high compressibility, low shear strength, and pronounced volume change behavior. These findings highlight the necessity for appropriate soil improvement measures or the adoption of alternative foundation design strategies to ensure structural stability and long-term performance.

Soils with high plasticity generally exhibit reduced workability and pronounced shrink–swell behavior, resulting in significant volumetric instability under moisture variation, as widely reported for expansive clay systems [7] and reflected in Table 5. The elevated plasticity index further indicates a high clay content with significant swelling potential, which can lead to reduced bearing capacity and an increased risk of foundation failure (Table 6). Although such soils may exhibit moderate shear strength in the dry state, their strength typically decreases considerably upon wetting, thereby contributing to structural instability [1].

The Casagrande plasticity chart (Figure 9), based on the Unified Soil Classification System (USCS), indicates that samples A, B, and C are classified as high plasticity clays (CH), while sample D falls within the intermediate plasticity clay (CI) category. High plasticity clays (CH) are characterized by high wa-

Table 3. Natural moisture content of soil samples compared with Nigerian Ministry of Works and Housing specifications [26, 34].

Sample	Weight of can (g)	Wet sample + can (g)	Dry sample + can (g)	Observed moisture content (%)	Recommended value (%)	Remark
A	109.16	327.95	286.92	23.08	5–15	Unsuitable
B	109.75	339.09	297.05	22.45	5–15	Unsuitable
C	141.02	362.11	324.54	20.47	5–15	Unsuitable
D	108.11	339.19	302.31	18.99	5–15	Unsuitable

Table 4. Consistency-limit test results and ensuing soil classification [28, 29].

Sample	Liquid limit, LL (%)	Plastic limit, PL (%)	Classification range of LL (%)	Plasticity class	Remark
A	56.80	15.65	50–70	High	Fat
B	55.50	20.87	50–70	High	Fat
C	53.00	14.10	50–70	High	Fat
D	49.00	17.93	35–50	Intermediate	Intermediate

Table 5. Sample classification based on plasticity index and potential expansiveness [28, 29].

Sample	PI (%)	PI classification (%)	Swelling potential
A	41.15	> 35	Very high
B	34.63	26–35	High
C	38.90	> 35	Very high
D	31.07	26–35	High

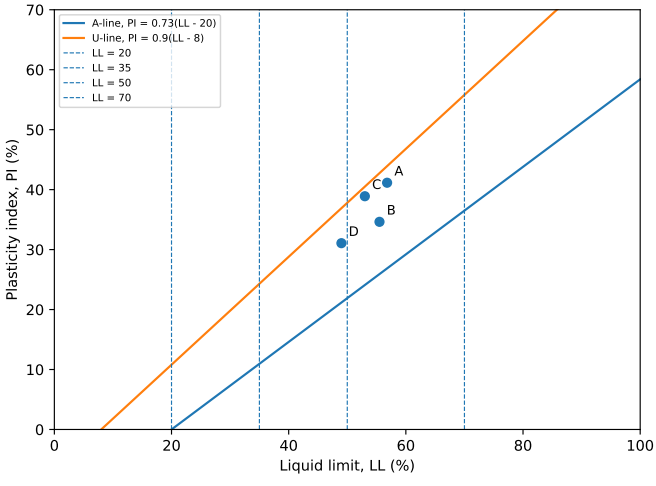


Figure 9. Casagrande plasticity chart showing classification of soil samples based on liquid limit and plasticity index.

ter retention capacity, low permeability, and a pronounced susceptibility to deformation under applied loads. These properties render them unstable and generally unsuitable for geotechnical applications without appropriate soil improvement measures [9] . Samples A, B, and C are therefore expected to undergo significant volumetric changes, including swelling during wet seasons and shrinkage during dry periods. Such behavior can adversely affect the integrity of foundations constructed on these soils [29] . Although sample D exhibits moderate plasticity (Figure 9), its relatively high swelling potential (Table 5) suggests that it still poses geotechnical challenges. Consequently, these characteristics may lead to poor drainage conditions, excessive settlement, and moisture accumulation around foundations, thereby increasing the risk of structural instability and reducing the long-term performance of infrastructure [3, 9].

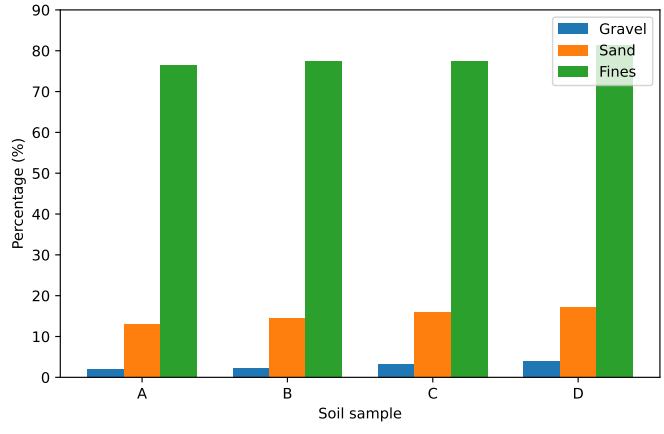


Figure 10. Percentage distribution of soil fractions showing dominance of fine-grained materials.

4.2.3. Undrained triaxial test

The undrained triaxial test results, as presented in Table 7, reveal notable variations in shear strength parameters among the soil samples. Sample A exhibits the highest cohesion value (22 kN/m^2), indicating relatively stronger interparticle bonding and improved undrained shear strength. In contrast, sample B shows the lowest cohesion (7 kN/m^2), reflecting weak bonding and reduced resistance to shear under undrained conditions [9, 29].

The angle of internal friction (ϕ) across all samples is very low, ranging from 1.53° to 5.07°, which is characteristic of saturated fine-grained soils [28, 29]. Under undrained conditions, particularly for saturated clays, the angle of internal friction is often assumed to be approximately zero, as shear strength is primarily governed by cohesion [35]. Consequently, higher cohesion generally corresponds to improved load-bearing capacity, as observed in Sample C, which exhibits a relatively higher bearing capacity (55.16 kN/m^2).

The bearing capacity of the soil samples ranges from 30.52 kN/m^2 to 55.16 kN/m^2. According to commonly applied geotechnical interpretation systems [28, 29], bearing capacity values greater than 100 kN/m^2 indicate good soil, 75–100 kN/m^2 indicate average soil, 40–75 kN/m^2 indicate poor soil, and values less than 40 kN/m^2 indicate very poor (bad) soil conditions. This suggests that the subsurface materials exhibit limited capacity for supporting structural loads under conventional shallow founda-

Table 6. Comparison of consistency-limit results for the study area with Nigerian Ministry of Works and Housing specifications [26, 34].

Soil property	Observed range (study area)	Recommended value	Remark
Liquid limit (%)	49.00–56.80	< 35	Unsuitable: exceeds limit; indicates high plasticity
Plastic limit, PL (%)	14.10–20.87	–	Informative only; no standard threshold
Plasticity index (%)	31.07–41.15	< 12	Unsuitable

Table 7. Undrained triaxial test results.

Soil sample	Cohesion (kN/m^2)	Angle of friction (ϕ°)	Bearing capacity (kN/m^2)
A	22	1.528	45.34
B	7	3.724	30.52
C	17	5.068	55.16
D	20	1.940	49.45

tion systems and would likely require ground improvement measures or alternative foundation designs to ensure stability and serviceability.

In summary, the observed ranges of cohesion, friction angle, and bearing capacity imply low to moderate shear strength, making the soils highly susceptible to deformation and instability under loading conditions [26, 28]. These geotechnical limitations likely contributed to the observed cases of structural failure and instability within the study area.

4.2.4. Consolidation test

Compressibility ranges from 0.0002475 m^2/kN (Sample A) to 0.0003100 m^2/kN (Sample B), the coefficient of consolidation varies between 0.2408 cm^2/min (Sample C) and 0.2590 cm^2/min (Sample A), while the coefficient of permeability ranges from 6.41×10^{-5} m/s (Sample A) to 7.51×10^{-5} m/s (Sample B).

According to established geotechnical consolidation principles [28, 29, 36],, soils with coefficients of volume compressibility between 0.0001 m^2/kN and 0.0003 m^2/kN exhibit medium compressibility, whereas values between 0.00031 m^2/kN and 0.0015 m^2/kN indicate high compressibility. In this study, the computed volume compressibility values indicate that the soils fall within medium to high compressibility ranges, suggesting a significant tendency for consolidation settlement and long-term deformation under structural loading.

The relatively low values of the coefficient of consolidation indicate a slow rate of dissipation of excess pore water pressure, which implies that settlement will occur gradually over an extended period [5, 7]. Furthermore, Eze *et al.* [1] reported that permeability values ranging from 10^{-6} to 10^{-4} m/s are considered moderate, 10^{-8} to 10^{-6} m/s as low, and 10^{-11} to 10^{-8} m/s as very low. The permeability values obtained in this study fall within the lower end of this spectrum, consistent with clay or silty clay materials characterized by low hydraulic conductivity [28]. Such soils typically exhibit poor drainage conditions and are prone to prolonged consolidation settlement, which may result in differential settlement and structural instability [28, 29]. These characteristics make the soils potentially unsuitable for direct foundation support without appropriate geotechnical improvement measures prior to construction.

4.2.5. Particle-size distribution (PSD)

The particle size distribution of a soil describes the relative proportions of different grain sizes; gravel, sand, silt, and clay, and is a fundamental parameter influencing soil behavior, classification, and geotechnical properties [28, 29]. The PSD results for Samples A, B, C, and D are presented in Table 9 and illustrated in Figure 10.

Across all samples, the fine-grained fraction predominates, ranging from 76.4% in Sample D to 81.4% in Sample A. This indicates that the soils are largely composed of silt- and clay-sized particles. A high fines content is typically associated with low permeability, high compressibility, and increased plasticity, which significantly influences their strength and deformation characteristics under applied loads.

The sand fraction is relatively low across the samples, varying between 10.98% (Sample A) and 13.36% (Sample D). Sand-sized particles contribute to improved drainage and mechanical interlocking, thereby enhancing shear strength and reducing the effects of plasticity [29]. However, the modest sand content observed suggests that the improvement in drainage and strength is limited, with the overall soil behavior still governed predominantly by the fine fraction.

Similarly, the gravel content is minimal, ranging from 2.10% to 3.92%. Gravel particles typically enhance load-bearing capacity and drainage by forming a stable coarse framework within the soil matrix [28, 29] . The low gravel percentages therefore indicate the absence of a well-developed coarse skeleton, further reinforcing the dominance of fine-grained, cohesive behavior in these soils.

The particle size distribution results corroborate the findings from the consistency limits and consolidation analyses, confirming that the soils are predominantly fine-grained, compressible, and likely to exhibit poor drainage and significant deformation under load. These characteristics further emphasize the need for appropriate geotechnical improvement measures prior to construction.

The descriptive statistical analysis of the particle size distribution (PSD) results for soil samples A, B, C, and D is presented in Table 10. The fine-grained fraction exhibits a very low coefficient of variation (2.70%), indicating a high degree of uniformity across the samples and suggesting relatively consistent depositional conditions within the study area. In contrast, the sand fraction shows moderate variability, while the gravel fraction, despite its low overall proportion, exhibits the highest relative variability. In general, the soils are predominantly fine-grained, indicating that their geotechnical behavior is largely controlled by this fraction. Such dominance is generally associated with low permeability, high compressibility, and predominantly cohesive mechanical behavior, conditions that may adversely affect drainage efficiency, bearing capacity, and settlement characteristics.

Finally, the geoelectrical and geotechnical results consistently indicate that the subsurface materials are predominantly fine-grained, highly plastic, compressible, and mechanically weak. These characteristics render the soils unsuitable for direct founda-

Table 8. Consolidation test results.

Consolidation parameter	A	B	C	D
Coefficient of compressibility (m^2/kN)	0.0002475	0.0003100	0.0002677	0.0002750
Coefficient of consolidation (cm^2/min)	0.2589516	0.2422783	0.240785	0.2494912
Coefficient of permeability (m/s)	0.0000641	0.0000751	0.0000650	0.0000686

Table 9. Summary of the particle-size distribution (PSD) of the soil samples.

Sample	Fine-grained soils (%)	Sand (%)	Gravel (%)
A	81.4	10.98	2.10
B	79.9	11.34	3.23
C	80.2	11.54	3.00
D	76.4	13.36	3.92

Table 10. Descriptive statistical summary of particle-size distribution (PSD) results for soil samples A, B, C, and D.

Statistic	Fine-grained (%)	Sand (%)	Gravel (%)
Mean	79.48	11.81	3.06
Standard deviation	2.15	1.06	0.75
Minimum	76.40	10.98	2.10
Maximum	81.40	13.36	3.92
Median	80.05	11.44	3.12
Range	5.00	2.38	1.82
Coefficient of variation (%)	2.70	8.99	24.53

tion support without appropriate ground improvement. Effective mitigation measures may include soil stabilization, provision of efficient drainage systems, or the adoption of alternative foundation designs to minimize the risks of excessive and differential settlement.

These findings are consistent with the geological setting of the area, which is extensively underlain by recent alluvial deposits associated with the Benue River floodplain. These unconsolidated sands, silts, and clays are typically water-saturated and laterally heterogeneous, and are therefore characterized by low shear strength, high compressibility, and elevated moisture content conditions that predispose foundations to instability and deformation [7, 37]. In addition, the influence of the underlying Precambrian Basement Complex, composed mainly of granites and gneisses, contributes to the formation of clay-rich regolith through weathering processes. This further modifies the geotechnical engineering behavior of near-surface materials, reinforcing the prevalence of weak, moisture-sensitive soils within the study area.

5. CONCLUSION

This study successfully integrated 2D electrical resistivity tomography (ERT) with comprehensive geotechnical laboratory analyses to diagnose the underlying causes of foundation failures within the heterogeneous basement complex terrain of northeastern Nigeria. The geoelectrical results consistently revealed very low resistivity values (2.67 – 24.7 Ωm), corresponding to water-saturated, clay-rich subsurface layers with varying degrees of soil corrosivity. These findings were strongly corroborated by geotechnical parameters, including high fines content (79.48%), elevated liquid limits (49.00–56.80%), high plasticity indices (31.07–41.15%), excessive natural moisture contents (18.99–23.08%), low undrained shear strength (7–22 kN/m^2), and low bearing capacity (maximum 55.16 kN/m^2). Consolidation characteristics further confirmed medium to high compressibility and low permeability, conditions conducive to differential settlement and long-term structural instability. The strong spatial agreement between low-resistivity anomalies and weak geotechnical properties establishes that foundation failure at the site is fundamentally controlled by saturated, highly plastic, and compressible clay horizons. These materials exhibit poor load-bearing performance and high susceptibility to volume change under fluctuating moisture regimes typical of floodplain and basement complex environments. The study demonstrates that integrated geophysical–geotechnical characterization provides a reliable predictive framework for identifying subsurface failure zones prior to construction. The findings underscore the necessity of adopting appropriate foundation systems, effective drainage control, and soil improvement measures in similar geological settings. Consequently, this work offers a practical and transferable model for sustainable foundation design and risk mitigation across moisture-sensitive clay terrains in northern Nigeria and comparable regions.

DATA AVAILABILITY

The data are available on request from the corresponding author.

DECLARATION OF COMPETING INTEREST

The authors declare that they have no known competing financial interests or personal relationships that could have appeared to influence the work reported in this manuscript.

FUNDING

This work did not receive any financial support in the form of funds or grants during the preparation of the manuscript.

References

[1] K. N. Eze, O. Igwe, D. N. Okereke, C. S. Uwom & K. P. Ukor, "Foundation integrity assessment of failed buildings in Ehamufu and Aguamede, South East Nigeria", Scientific Reports **13** (2023) 719. https://doi.org/10.1038/s41598-023-28043-y.

[2] K. Sudha, M. Israil, S. Mittal & J. Rai, "Soil characterization using electrical resistivity tomography and geotechnical investigations", Journal of Applied Geophysics **67** (2009) 74. https://doi.org/10.1016/j.jappgeo.2008.09.012.

[3] A. Devi, M. Israil, R. Anbalagan & P. K. Gupta, "Subsurface soil characterization using geoelectrical and geotechnical investigations at a bridge site in Uttarakhand Himalayan region", Journal of Applied Geophysics **144** (2017) 78. https://doi.org/10.1016/j.jappgeo.2017.07.005.

[4] J. Audu, E. Ike, J. B. Yerima & A. S. Oniku, "Geophysical investigation of road pavement failure along the Mubi Bypass Road, Jambutu, Jimeta, Yola, Adamawa State", Nigerian Journal of Physics **34** (2025) 28. https://njp.nipngr.org/index.php/njp/article/view/369.

[5] A. O. Atilade, J. O. Coker & N. O. Adebisi, "Integrated geophysical and geotechnical methods for pre-foundation investigations at Lagos State University of Science and Technology, Ikorodu, Southwestern Nigeria", Nige-

rian Journal of Physics **33** (2024) 134. https://doi.org/10.62292/njp.v33(s).2024.261.

[6] N. Aguirre-Macias, M. Fuentes-Arreazola, S. Pedroza-Ruciles, H. Rendon-Contreras & J. Chavoya-Gama, ''Subsurface geotechnical-characterization near some buildings at the Centro Universitario de la Costa UDG (Puerto Vallarta, Jalisco, Mexico) using electrical resistivity tomography'', Open Journal of Civil Engineering **14** (2024) 520. https://doi.org/10.4236/ojce.2024.144029.

[7] F. Oppong & O. Kolawole, ''Reassessment of natural expansive materials and their impact on freeze–thaw cycles in geotechnical engineering: a review'', Frontiers in Built Environment **10** (2024) 1396542. https://doi.org/10.3389/fbuil.2024.1396542.

[8] P. M. Soupios, P. Georgakopoulos, N. Papadopoulos, V. Saltas, A. Andreadakis, F. Vallianatos & J. P. Makris, ''Use of engineering geophysics to investigate a site for a building foundation'', Journal of Geophysics and Engineering **4** (2007) 94. https://doi.org/10.1088/1742-2132/4/1/011.

[9] A. Sharma, M. Samanta & D. P. Kanungo, ''Site-specific correlation between geotechnical and geoelectrical properties of soil deposits in India'', Journal of Applied Geophysics **221** (2024) 105288. https://doi.org/10.1016/j.jappgeo.2024.105288.

[10] M. S. Erick, K. S. Parfait & B. Dieudonne, ''Geophysical investigations of heterogeneity foundation soils using electrical resistivity tomography technique'', Soil Mechanics and Foundation Engineering **61** (2025) 592. https://doi.org/10.1007/s11204-025-10016-0.

[11] M. H. Loke & R. D. Barker, ''Practical techniques for 3D resistivity surveys and data inversion'', Geophysical Prospecting **44** (1996) 499. https://doi.org/10.1111/j.1365-2478.1996.tb00162.x.

[12] M. H. Loke, J. E. Chambers, D. F. Rucker, O. Kuras & P. B. Wilkinson, ''Recent developments in the direct-current geoelectrical imaging method'', Journal of Applied Geophysics **95** (2013) 135. https://doi.org/10.1016/j.jappgeo.2013.02.017.

[13] A. Samouelian, I. Cousin, A. Tabbagh, A. Bruand & G. Richard, ''Electrical resistivity survey in soil science: a review'', Soil and Tillage Research **83** (2005) 173. https://doi.org/10.1016/j.still.2004.10.004.

[14] A. I. Obasi, O. P. Aghamelu, C. N. Chukwu & P. N. Nnabo, ''Engineering geophysical study of the Ebonyi State University permanent site, Abakaliki, South-Eastern Nigeria'', Current Journal of Applied Science and Technology **7** (2015) 168. https://doi.org/10.9734/BJAST/2015/15195.

[15] O. A. Odundun, V. I. Fagorite & E. O. Rogbitan, ''Geoelectrical and geotechnical investigation of foundation failure in and around Oroke High School, Akungba-Akoko, southwestern Nigeria'', International Journal of Advanced Geosciences **8** (2020) 237. https://doi.org/10.14419/ijag.v8i2.31121.

[16] F. Bellmunt, A. Gabas, A. Macau, B. Benjumea, M. Vila & S. Figueras, ''Sediment characterization in deltas using electrical resistivity tomography: the Ebro delta case'', Journal of Applied Geophysics **196** (2022) 104520. https://doi.org/10.1016/j.jappgeo.2021.104520.

[17] O. Adewoyin, E. O. Joshua, I. I. Akinwumi, M. Omeje & E. S. Joel, ''Evaluation of geotechnical parameters using geophysical data'', Journal of Engineering and Technological Sciences **49** (2017) 95. https://doi.org/10.5614/j.eng.technol.sci.2017.49.1.6.

[18] W. Lowrie, Fundamentals of Geophysics, 2nd ed. Cambridge University Press, Cambridge, UK, 2007, pp. 66–70. https://doi.org/10.1017/CBO9780511807107.

[19] W. M. Telford, L. P. Geldart & R. E. Sheriff, Applied Geophysics, 2nd ed., Cambridge University Press, Cambridge, UK, 1990, pp. 353–358. https://doi.org/10.1017/CBO9781139167932.

[20] J. Benkhelil, ''The origin and evolution of the Cretaceous Benue Trough (Nigeria)'', Journal of African Earth Sciences (and the Middle East) **8** (1989) 251. https://doi.org/10.1016/S0899-5362(89)80028-4.

[21] N. G. Obaje, Geology and Mineral Resources of Nigeria, Springer, Berlin, Germany, 2009. https://doi.org/10.1007/978-3-540-92685-6.

[22] M. A. Olade, ''Evolution of Nigeria's Benue Trough (aulacogen): a tectonic model'', Geological Magazine **112** (1975) 575. https://doi.org/10.1017/S001675680003898X.

[23] Adamawa State Government, The 2012 Flood Report, Ministry of Environment, Adamawa State, Nigeria, 2012.

[24] M. A. Olade, ''Early Cretaceous basalt volcanism and initial continental rifting in Benue Trough, Nigeria'', Nature **273** (1978) 458. https://doi.org/10.1038/273458a0.

[25] H. S. Ward, ''Resistivity and induced polarization methods'', in Geotechnical and Environmental Geophysics, S. H. Ward (Ed.), Society of Exploration Geophysicists, Houston, USA, 1990, pp. 147–189. https://doi.org/10.1190/1.9781560802785.

[26] I. A. Akinlabi & C. O. Adegboyega, ''Engineering geophysical investigation of road failure in a basement complex terrain, Southwestern Nigeria'', Journal of Geography, Environment and Earth Science International **25** (2021) 40. https://doi.org/10.9734/JGEESI/2021/v25i230270.

[27] M. A. Abed, A. A. A. Othman, S. Shebl, M. Zayed & M. H. Farag, ''A comprehensive geotechnical and geophysical assessment of the foundation sublayers in Egypt's New Administrative Capital'', Scientific Reports **15** (2025) 43229. https://doi.org/10.1038/s41598-025-29246-1.

[28] H.-Y. Fang & J. L. Daniels, Introductory Geotechnical Engineering: An Environmental Perspective, CRC Press, Boca Raton, USA, 2006. https://doi.org/10.1201/9781315274959.

[29] J.-L. Briaud, ''Introduction in geotechnical engineering'', in Geotechnical Engineering: Unsaturated and Saturated Soils, J.-L. Briaud (Ed.), Wiley, Hoboken, USA, 2023. https://doi.org/10.1002/9781119788720.ch1.

[30] S. A. Bisong, A. A. Abong & A. O. Egor, ''Geophysical investigation of pavement failure along Jonathan By-Pass–Akansoko and Atimbo–Parliamentary roads in Calabar metropolis, Cross River State, Nigeria'', Science World Journal **18** (2023) 375. https://doi.org/10.4314/swj.v18i3.8.

[31] A. I. Idornigie & M. O. Olorunfemi, ''Electrical resistivity determination of subsurface layers, subsoil competence and soil corrosivity at an engineering site location in Akungba Akoko, South Western Nigeria'', Ife Journal of Science **8** (2006) 159. https://doi.org/10.4314/ijs.v8i2.32216.

[32] I. A. Akinlabi & M. L. Olaiya, ''Geoelectrical and physicochemical evaluation of soil corrosivity on metallic pipelines: a case study'', Journal of Geography, Environment and Earth Science International **25** (2021) 46. https://doi.org/10.9734/JGEESI/2021/v25i530287.

[33] A. H. Amadi, J. A. Ajienka, O. Akaranta, P. R. Moses, N. U. Achara, V. D. Ola & R. D. Udo, ''A review of soil resistivity testing for enhanced corrosion control: overcoming limitations through integrated geophysical approaches and alternative methodologies'', Measurement **242** (2025) 116214. https://doi.org/10.1016/j.measurement.2024.116214.

[34] J. O. Irokwe, I. L. Nwaogazie & S. Sule, ''Development of empirical models for the estimation of CBR value of soil from their index properties: a case study of the Ogbia-Nembe Road in Niger Delta Region of Nigeria'', Open Journal of Civil Engineering **12** (2022) 648. https://doi.org/10.4236/ojce.2022.124036.

[35] R. Glossop & A. W. Skempton, ''Particle-size in silts and sands'', Journal of the Institution of Civil Engineers **25** (1945) 81. https://doi.org/10.1680/ijoti.1945.13927.

[36] K. H. Head & R. J. Epps, *Manual of soil laboratory testing, Volume II, Permeability, Shear Strength and Compressibility Tests*, 3rd ed. Caithness, Scotland: Whittles Publishing. https://archive.org/details/manualofsoillabo0000head_p8s3.

[37] E. Ike, J. Park, R. Ewusi-Wilson & C. Lee, ''Chemo-mechanical controls on clay fabric: generalized maps for predicting soil behavior in variable chemical environments'', Next Sustainability **7** (2026) 100296. https://doi.org/10.1016/j.nxsust.2026.100296.